Available online at www.sciencedirect.com
SCIENCE DIRECT®
Nuclear Instruments and Methods in Physics Research A 499 (2003) 45–65
NUCLEAR INSTRUMENTS & METHODS IN PHYSICS RESEARCH Section A
www.elsevier.com/locate/nima

RF systems for the KEK B-Factory

K. Akai[a], N. Akasaka[a], K. Ebihara[a], E. Ezura[a,*], T. Furuya[a], K. Hara[a], K. Hosoyama[a], S. Isagawa[a], A. Kabe[a], T. Kageyama[a], Y. Kojima[a], S. Mitsunobu[a], H. Mizuno[a], Y. Morita[a], H. Nakai[a], H. Nakanishi[a], M. Ono[a], H. Sakai[a], M. Suetake[a], T. Tajima[b], Y. Takeuchi[a], Y. Yamazaki[a], S. Yoshimoto[a]

[a] *KEK, High Energy Accelerator Research Organization, 1-1 Oho, Tsukuba, Ibaraki 305-0801, Japan*
[b] *Los Alamos National Laboratory, USA*

Abstract

This paper describes the design features and operational status of the RF systems for the KEK B-Factory (KEKB). Two types of new RF cavities have been developed to store very high-intensity beams with many short bunches. The design and performance of the cavities and other critical components, such as the input couplers and HOM dampers, are reported. The configuration of the RF systems is given and descriptions of various control loops are made, including a direct RF feedback loop and a 0-mode damping loop. The effects of transient beam loading due to a bunch gap on bunch phase modulations were simulated and measured. The development of a superconducting crab cavity, which is a component of luminosity upgrade strategy, is also presented.
© 2002 Elsevier Science B.V. All rights reserved.

PACS: 29.20

Keywords: Accelerator; B-factory; RF system; RF control; Accelerating cavity; Crab cavity

1. Introduction

The KEKB is a high-luminosity asymmetric electron–positron collider optimized for the study of CP violation [1]. It consists of an 8 GeV high-energy ring (HER) for electrons and a 3.5 GeV low-energy ring (LER) for positrons. The installation of the machine was completed in October 1998, and the first electron beam was stored in the HER on December 1, 1998. Since the first hadronic events were observed in the Belle detector at the beginning of June 1999, the luminosity of KEKB has been steadily increased, reaching 4.49×10^{33} cm^{-2} s^{-1} in July 2001.

The KEKB RF system has been designed to store electron and positron beam currents of 1.1 and 2.6 A, respectively. The large circulating currents make it imperative to keep the higher-order mode (HOM) impedance of the cavity as low as possible to avoid uncontrollable coupled-bunch instabilities. Serious problems common to B-factories are the excitation of fast growing longitudinal coupled-bunch instabilities by the accelerating mode of significantly detuned RF cavities,

*Corresponding author. Tel.: +81-298-64-1171; fax: +81-298-64-3182.
E-mail address: ezura@post.kek.jp (E. Ezura).

0168-9002/03/$ - see front matter © 2002 Elsevier Science B.V. All rights reserved.
PII: S0168-9002(02)01773-4

and transient beam loading due to a bunch gap, which causes phase variations of bunches along a bunch train. In order to overcome these difficulties, two types of innovative HOM-damped cavities with large stored energy have been developed, i.e., a normal conducting three-cavity system (ARES) [2] and a single-cell superconducting cavity (SCC) [3]. An increase in the stored energy per cavity decreases the detuning of the cavity, which makes it possible to reduce the growth rate of the coupled-bunch instability below the radiation damping rate. A decrease in the cavity detuning can also reduce the effects of bunch-gap transients to such a small level that no other measures are necessary. Since the ARES has a larger stored energy and is consequently more suitable for reducing cavity detuning, ARES alone is used for the LER where the beam loading is heavier. The HER, where a higher RF voltage is required, is equipped with a combination of the SCC and the ARES. They are operated with a suitable relative phase-angle to assign higher cavity voltage to the SCC and heavier beam loading/Vc to the ARES.

Most of the high-power RF components, such as klystrons, circulators and waveguides, were taken from TRISTAN as well as the low-level RF control modules. The RF system and its components have been thoroughly re-examined and improved in order to cope with heavy beam loading and to meet the increased demands associated with high luminosity. A variety of new feedback loops have been incorporated into the existing RF system to stabilize the RF and its interaction with the beam.

2. System overview

The choice of RF frequency was influenced by the needs to reuse the TRISTAN RF components and to minimize the injection jitter. The former requires that the RF frequency be in the range of ± 0.3 MHz from the TRISTAN frequency, which is the operational frequency range of the klystron. The latter suggests that the ring RF frequency be phase locked to the linac RF frequency, which is accomplished if each frequency is a multiple of a common subharmonic frequency. We selected a frequency of 508.887 MHz to meet these needs.

Table 1
RF-related machine parameters and design RF parameters

Parameter	LER	HER
Beam energy (GeV)	3.5	8.0
Beam current (A)	2.6	1.1
Energy damping time (ms)	23	23
Radiation loss (MV)	1.6	3.5
Beam power (MW)	4.5	4.0
Bunch length (mm)	4	4
RF frequency (MHz)	508.887	508.887
Harmonic number	5120	5120
Cavity type	ARES	SCC/ARES
Number of cavities	20	8/12
Relative phase (deg)	—	10
Total RF voltage (MV)	10	17.9
R/Q of cavity (Ω)	14.8	93/14.8
Loaded Q of cavity ($\times 10^4$)	3.0	7.0/3.0
Coupling factor	2.7	$2.8 \times 10^4/2.7$
RF voltage/cavity (MV)	0.5	1.5/0.5
Wall loss/cavity (kW)	154	—/154
Beam power/cavity (kW)	221	240/173
Input power/cavity (kW)	375	250/340
Number of klystrons	10	8/6
Klystron power (kW)	$\sim$810	$\sim$270/$\sim$730

A high-power RF system for the generation and distribution of power consists of a 1 or 1.2 MW klystron, its power supply (PS), a 1 MW circulator, a 1.2 MW water load, WR-1500 waveguide components, etc. A CW 1.2 MW water-load has been developed for the KEKB to absorb the beam-induced power, which can be more than 1 MW when a klystron trips off at the full beam current [4]. For reuse in KEKB, various improvements and modifications have been given to the klystrons to obtain characteristics upgrading and higher stability [5,6]. The klystron PSs have been improved to eliminate any false firing of the crowbar circuit, which had been a long-standing problem in TRISTAN operation [7].

Table 1 gives the RF-related machine parameters and the design RF parameters. The LER is now equipped with 8 klystron stations and 16 ARESs; each of the two ARESs driven by one klystron. The HER now has 13 klystron stations, of which 5 klystrons drive 10 ARESs and 8 klystrons drive 8 SCCs. The present number of

cavities can support a LER beam current of 1.8A and a HER beam current of 1.0 A. However, the usual beam currents are presently limited to 0.96 and 0.78 A, respectively, mainly due to beam blow-up problems in LER and heating of the beam-line components by HOM as well as synchrotron radiation power in HER. To achieve the design beam currents, four more ARESs will be added to the LER and two more ARESs to the HER in the summer of 2002.

3. Low-level control system

3.1. RF distribution and stabilization

The RF phase of every station in both rings should be accurately controlled. Any phase error of one ring relative to the other gives rise to a displacement of the colliding point. For KEKB, with a short bunch length and small β^*, even a small phase error reduces the luminosity, due to the hour-glass effect. Furthermore, a phase error in one cavity relative to the other cavities in the same ring causes extra input power to that cavity to keep the cavity voltage constant, due to the heavy beam-loading.

The RF signal from the master oscillator is provided for the RF stations via the RF reference lines shown in Fig. 1. Each segment of the reference line is phase stabilized by its own independent feedback system, which uses a second subharmonic signal returned from the end of each line [8]. Two independent reference lines are used; one reference line transmits the RF signal clockwise, and the other counterclockwise. The phase difference between the two lines are always monitored at two stations (D1 and D7), diagonal to each other in the ring. The phase error around the ring is held at less than 1°.

Although the phase shift due to a temperature change or other slow drift is stabilized by the feedback loops in the reference line, random 0-mode synchrotron beam oscillations of about $\pm 0.5^\circ$ were observed at the beginning of the commissioning, even at a very low beam current. The oscillation was not caused by a beam instability, but by some low-frequency noise in the driving system. In order to damp the oscillation, a 0-mode damping system was installed. The beam signal, picked up by a button electrode, is transmitted to a high-Q cavity filter to obtain the RF frequency component. Both the beam signal and the reference RF signal are down-converted to 5 MHz and their relative phase is detected. The phase error is transmitted to a band-pass filter centered at about 1 kHz to detect the synchrotron oscillation. After rotating it by 90°, it is fed to the ring phase shifter. With the damper, the 0-mode beam oscillation is sufficiently reduced down to ± 0.05–0.1°.

For a large circumference ring with a high beam current, longitudinal coupled-bunch instabilities of the $\mu = -1, -2, -3$ modes, and so on, can be strongly excited due to a large detuning for the high-current beam. In KEKB, however, the large stored energy of the ARES and SCC reduces the detuning frequency by an order of magnitude. In the present operation it is $5 \sim 10$ kHz, much smaller than the revolution frequency of 99.4 kHz, and no sign of an instability has been observed. Nevertheless, the growth time with the design beam current in LER for the $\mu = -1$ mode is 15 ms at $V_c = 10$ MV or 7 ms at 5 MV, which is faster than the radiation damping time of 20 ms. A feedback system using a digital band-pass filter centered at the frequency $f_{rf} - f_{rev} + f_s$ has been developed [9], where f_{rf} and f_{rev} are the RF frequency and the revolution frequency, respectively. It will be introduced for higher beam current.

3.2. RF station control

3.2.1. Amplitude and phase control loops

A block diagram of one RF station for SCC is shown in Fig. 2 [10]. An RF station for the ARES is basically the same, except for 2 cavities/1 klystron configuration and a tuning control system specific to the ARES. In addition to the cavity feedback loops, klystron feedback loops are implemented to stabilize the amplitude and phase of the klystron output. They reduce any phase variations due to cathode voltage variations, and eliminate power supply ripples and noise around the synchrotron frequency. A

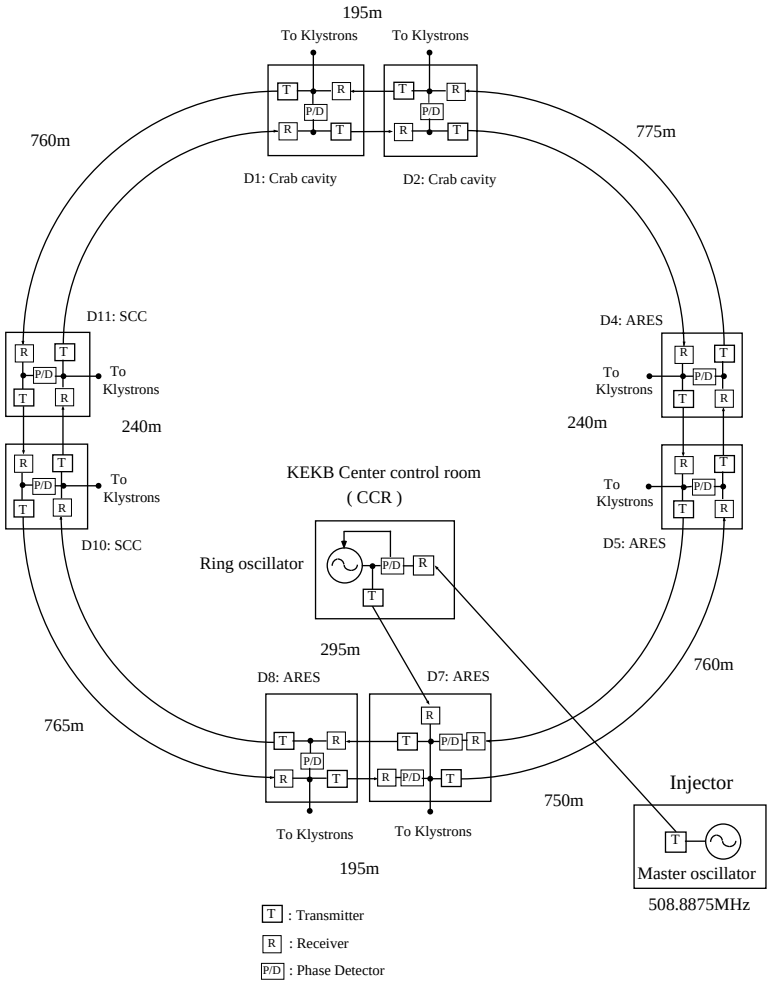

Fig. 1. Distribution of the RF signal from the master oscillator.

direct RF feedback around the RF frequency is implemented to reduce any beam-loading effects on the RF system and to improve the beam stability. Prior to the construction of KEKB, a direct feedback was tested in the TRISTAN AR in 1996. It was proved to be effective in damping the $\mu = 0$ mode oscillation and improving the beam stability concerning the static Robinson criteria [11].

3.2.2. *Tuning control system*

The ARES should be operated in such a way that the resonant frequency of the accelerating cavity is detuned to compensate for the reactive component of the beam loading, while that of the energy-storage cavity is kept at the operating frequency. This condition is necessary not only for power minimum operation under beam loading, but also for distributing energy properly between the three cavities. In particular, if a high field is accidentally excited in the coupling cavity due to a tuning error, the damper attached at the coupling cavity can be damaged. After studying the tuning accuracy and stability of several possible methods [12], the tuning system was determined to be as shown in Fig. 3. Under normal operation, the phase of the energy-storage cavity is locked to that of the incident RF, and the

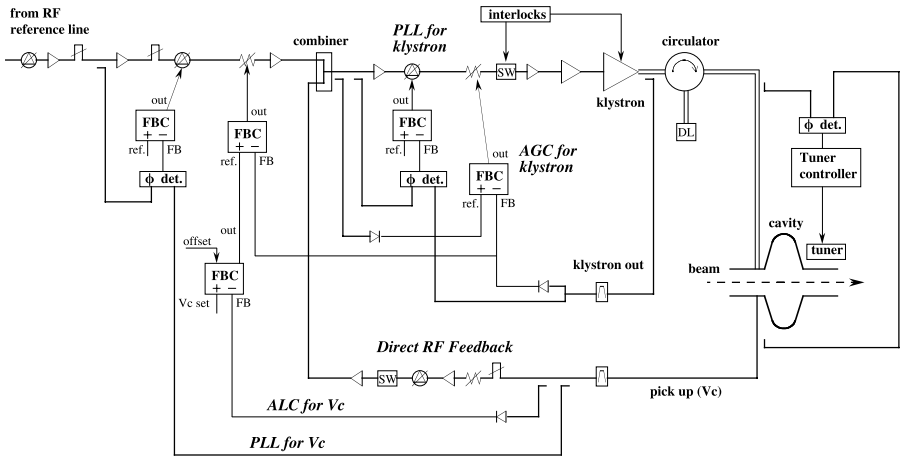

Fig. 2. RF station for the SCC cavities.

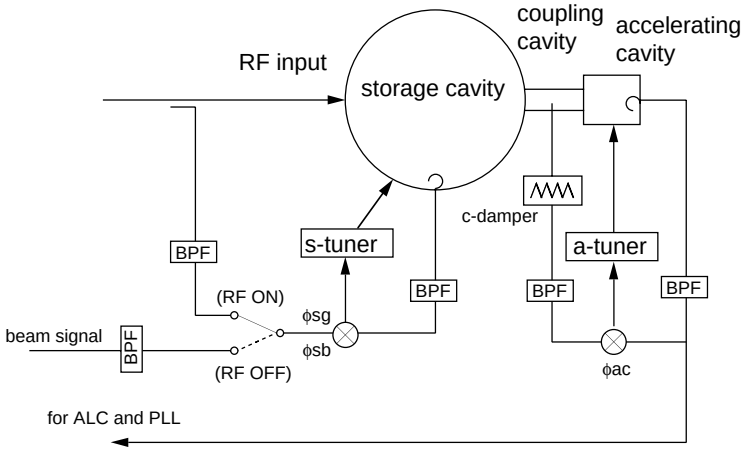

Fig. 3. Tuning control.

phase of the accelerating cavity to the coupling cavity.

When an RF station operating at nominal power is tripped off, the resonant frequency of the ARES tends to decrease at first by about 100 kHz in about 80 s, and then turns to increase if no tuning control is applied. This is caused by the thermal deformation properties of the end plates of the storage cavity. In order to avoid the $\mu = -1$ mode instability caused by tripped cavities and a large amount of beam-induced power, that can damage the cavity or the high-power system, the frequency of the tripped cavities is automatically kept between f_{rf} and $f_{rf} - f_{rev}$, about -30 kHz away from f_{rf}. It is done by controlling the storage cavity tuner according to the relative phase between the beam signal and the beam-induced voltage. When the cavity trips, the reference signal for the energy-storage cavity is switched from the incident RF to the beam signal [10].

3.3. Protection against trips

3.3.1. Trips and recovery

The RF system is designed so that an ARES station can trip without any beam loss, and that the tripped station can be turned on again without losing a high-current stored beam, after the

trouble is cleared. Considering the trip rate and refilling time, it contributes to improve the integrated luminosity. This is done as follows: (1) Even when an ARES station trips, a sufficiently high RF voltage is still provided by other operating stations. The shift of the collision point due to the voltage change is compensated for by shifting the RF phase. (2) As described above, the resonant frequency of the tripped ARES is controlled at a safe frequency between f_{rf} and $f_{rf} - f_{rev}$. (3) The tripped station is turned on again with carefully designed parameters and control sequence, which minimizes any disturbance to the turned-on RF station and the beam.

3.3.2. *Beam phase abort*

In operation with a high-current beam, it turned out that a trip of two ARES stations at the same time, or, even one SCC station, sometimes causes a large effect on the beam-line hardware components: A large amount of radiation hit the Belle detector, the worst case of which was 5 krad at one occasion. In addition, some of the problems of vacuum components may be attributed to damage caused by a lost beam. It is understood that the trip varies the beam energy by more than 0.5%, which results in a large transverse orbit drift. Although some interlock signals are connected to a beam-abort system, it does not help in all cases; the accelerating field in the cavity can become abnormal before detecting any interlock signals. A trip of the SC cavity also results in a helium pressure rise and the evaporation of a large amount of helium, which takes about 10 min to recover to the normal operating condition. This is because the quench continues due to the beam-induced power, even if the driving RF is switched off by a quench detector or arc sensors.

Recently, a new protection system was installed. It detects the beam phase relative to the RF phase and generates a request signal to the beam abort system when the beam phase deviates from a normal range. Then, the beam is aborted within 160 μs. (This delay is generated in the abort system and is expected to be reduced.) After this system was installed, no big radiation has hit the Belle detector when the RF trips. Also, the helium pressure is kept stable when a quench of the SC cavity occurs.

4. Bunch gap transient

A part ($10\% \simeq 1$ μs) of each ring is not filled with bunches so as to allow for the rise time of the beam-abort kicker. It also works as an ion-clearing gap in the HER. The amplitude and phase of the accelerating voltage is modulated by the bunch gap, since the beam-loading effect is different between the gap and the beam. As a result, the longitudinal synchronous position is shifted bunch-by-bunch along the train. The modulation was calculated bunch by bunch and turn-by-turn in the time domain using a simulation code, which had been developed to study the beam-cavity system of KEKB, including the feedback loops [10].

The phase shift along a train is measured during a collision using a gated bunch-by-bunch beam-monitor system [13]. The measured phase shift is shown in Fig. 4 together with the simulation result. They are quantitatively in good agreement, except at the leading part of the train before the bucket number of about 401. The reason for the rapid increase at the leading part of the train may be due to some longitudinal wake within a range shorter than 400 buckets, which was not taken into account in the simulation, or may be due to insufficient isolation or other imperfection of the gate module.

So far, the phase modulation is relatively small, owing to the large stored energy in the ARES and SCC, and lower beam current than the design current. The collision point shift is smaller than the present bunch length of 6 mm, and no luminosity reduction is attributed to the phase modulation. At the design beam current of 2.6 A in the LER and 1.1 A in the HER, and the design bunch length of 4 mm, however, the phase modulation may cause luminosity reduction. A simulation result for the design current is summarized in Table 2. It is foreseen that the gap length will be reduced from 10% to 5% in the future.

It should also be noted that the response of the coupling cavity of the ARES is very fast, since it

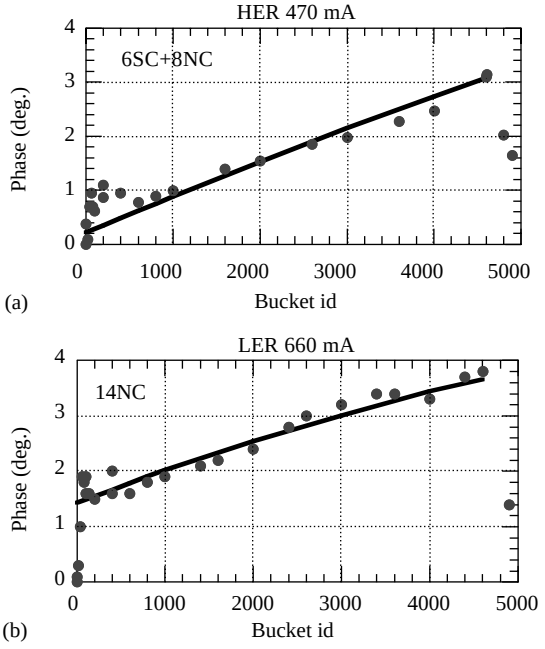

Fig. 4. Phase shift along the bucket position.

Table 2
Bunch position shift due to a 10% gap in both rings

	LER	HER
Current (A)	2.6	1.1
Phase modulation (p-p) (degree)	7.0	5.4
Δz (p-p) (mm)	11.4	8.8
Δz (relative)[a] (mm)	± 0.65	

[a] $(\Delta z_{her} - \Delta z_{ler})/4$.

has a damper to reduce the Q-value of the coupling cavity to about 50. In the LER, the extracted power from the coupling cavity changes from 4 kW in the bunch train to 77 kW at the gap with an average power of 8 kW at the design beam current.

5. Operating status

Table 3 shows history of upgrading the RF system. The commissioning started with 12 ARES cavities in the LER and 6 ARES and 4 SC cavities in the HER. The number of cavities has been increased to meet higher beam currents. Since October 2000, the LER has been operated with 14 ARESs and the HER with 8 ARESs and 6 SCCs.

Table 3
Number of cavities and RF stations since commissioning

	LER	HER	
	ARES	ARES	SCC
December 1998 ~	12 (6)	6 (3)	4 (4)
October 1999 ~	16 (8)	10 (5)	4 (4)
October 2000 ~	16 (8)	10 (5)	8 (8)
In operation in 2001	14 (7)	8 (4)	6 (6)
Design	20 (10)	12 (6)	8 (8)

Table 4
Achieved and design parameters as of June 2000

	LER	HER	
	ARES	ARES	SCC
Beam current (mA)	1030 (2600)	872 (1100)	
Operating voltage (MV)	6 (5 ~ 10)	11 (10 ~ 18)	
No. of cavities	16 (20)	10 (12)	8 (8)
Voltage/cav. (MV)	0.43	0.34	1.38
(conditioned up to)	0.5 (0.5)	0.45 (0.5)	> 2.0 (1.5)
Total Beam power (MW)	1.8 (4.5)	3.0 (4.0)	
Beam power/cav. (kW)	130	200	380
(by shifting RF phase)	170 (225)	250 (170)	(250)
HOM power/cav. (kW)	2.0		7.5 (5.0)

Numbers in () are design values.

5.1. Cavity performance

Table 4 shows the present operating status of the RF system. The stored beam current has been increased up to 1030 mA in the LER and 872 mA in the HER. So far, the beam current has never been limited by the RF system. The potential current limitation due to the RF system is approximately proportional to the number of cavities, i.e. the power to be delivered to the beam: The present RF system could support 1.8 A in the LER and 1 A in the HER.

The SCC delivered a beam power of 380 kW per cavity, which is much more than the design value. The delivered beam power by the ARES in the HER has achieved the design value. Although the beam power by the ARES in the LER has been relatively low due to the current limitation, mainly caused by the photo-electron instability, the property has been tested up to 170 kW per cavity. This was done by shifting the RF phase of each cavity one by one so that much larger power is delivered by the cavity.

The HOM dampers, made of SiC for the ARES and ferrite for the SCC, have been working well. Up to 7.5 kW power has been absorbed by the ferrite damper per cavity. No sign of coupled-bunch instabilities caused by HOM's of the cavities has been observed.

5.2. System reliability

The RF system has been stably operated for physics runs; the frequency of the beam loss or machine down time due to RF problems is small. The total loss time due to any RF problems is 84 h for 8 months operation from October 2000 to July 2001. The number of beam aborts due to RF trips is about 130 in 5 months operation from February to June 2001. The average frequency is about once per day. The longitudinal collision point is kept stable, and no luminosity degradation has been attributed to the RF system.

6. Normal conducting cavity (ARES)

6.1. Design features

The operation of conventional copper cavities under heavy beam-loading conditions would give rise to a serious problem with longitudinal coupled bunch instabilities driven by the accelerating mode, whose resonant frequency is usually detuned toward the lower side from the RF frequency in order to compensate for the reactive component of the beam-induced cavity voltage. In 1991, Funakoshi [14] first pointed out that a cavity structure with a smaller R/Q is preferable to cure this problem. This is equivalent to increasing the ratio of the electromagnetic energy stored in the cavity over the interaction energy between the accelerating field and the beam current. In order to reduce the R/Q value by an order of magnitude, Shintake [15] proposed two schemes by using a cylindrical energy storage cavity operated in the high-Q TE_{015} mode. One scheme is a two-cavity system in which an accelerating cavity is directly coupled to a storage cavity, like the LEP normal conducting cavity [16]. The other is a more complicated one in which two accelerating cavities are coupled with two storage cavities via a four-port 3 dB coupler. However, either scheme is inconclusive to present no clear solution, even to the following fundamental problems with coupled-cavity systems operated under heavy beam loading conditions. The first problem is how to do well both in adjusting the ratio of the electromagnetic energy in the storage cavity to that in the accelerating cavity, and in keeping this energy ratio stable in amplitude and phase under heavy beam-loading conditions. The second problem is how to cure a beam instability due to the parasitic mode(s) emerging in coupled-cavity schemes without deteriorating the accelerating mode. However, this selective cure may not be easy because the accelerating mode can become a parasitic mode, and vice versa, when the viewpoint is changed.

The first feasible conceptual model satisfying the fundamental requirements stated above is a three-cavity system proposed by Yamazaki and Kageyama [17]. This is a coupled-cavity system operated in the $\pi/2$ mode, in which an accelerating cavity is resonantly coupled with an energy storage cavity via a coupling cavity equipped with a parasitic mode damper against the 0 and π modes. This coupled-cavity system was later named ARES, which is an acronym for Accelerator Resonantly coupled with Energy Storage. The resonant coupling in the $\pi/2$-mode enables the following key design features of the ARES cavity system:

- The $\pi/2$ mode is most stable against tuning errors and heavy beam-loading conditions.
- The stored energy ratio, $U_a : U_s$, where U_a is the stored energy in the accelerating cavity and U_s in the storage cavity, can be easily adjusted by changing the coupling factor ratio, $k_a : k_s$,

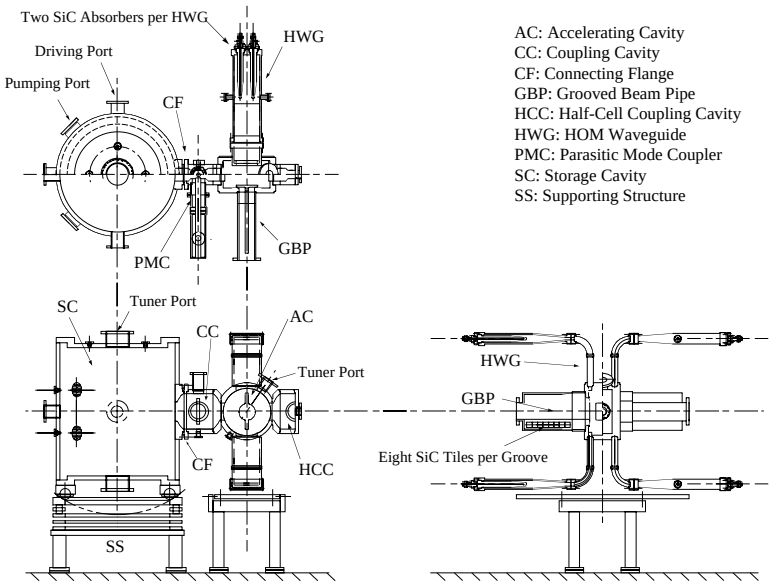

Fig. 5. A schematic drawing of the ARES cavity system.

where k_a is the coupling factor between the accelerating and coupling cavities and k_s is that between the storage and coupling cavities.

- The parasitic 0 and π modes can be selectively damped with an antenna-type coupler installed into the coupling cavity. Furthermore, the damped 0 and π modes are located nearly symmetrically with respect to the $\pi/2$ mode. Therefore, those impedance contributions to beam instabilities can be adjusted so as to cancel out each other.
- The coupling cavity functions as a filter to isolate the storage cavity from HOM's of the accelerating cavity.

6.2. RF structure including accessory devices

Fig. 5 shows a schematic drawing of the ARES cavity for KEKB. The design is based on a conceptual demonstrator named ARES96 [18] with an energy storage cavity operated in the TE_{013} mode. The change to the TE_{013} mode [19] is a compromise with the available space in the KEKB tunnel. The major RF parameters are listed in Table 5. The stored energy ratio $U_a : U_s$ is set at 1:9, and the design cavity voltage of 0.5 MV is generated with a wall dissipation of 150 kW in total, 60 and 90 kW inside the accelerating and storage cavities, respectively. The accelerating cavity, itself, is a HOM-damped structure made mainly of Oxygen Free Copper (OFC) parts brazed stepwise in a vacuum furnace. The accelerating cell is a kind of pillbox cavity with 10-mm-high nosecones. The cell structure was designed to be as simple as possible from the viewpoint of structural stability in thermal deformation rather than increasing the shunt impedance. Four straight rectangular waveguides are directly brazed to the upper and lower sides of the accelerating cavity in order to damp monopole HOM's and dipole ones deflecting the beam in the vertical direction. The waveguide width was chosen 240 mm, which gives a cut-off frequency of 625 MHz for the TE_{10} wave. The extracted

Table 5
Major RF parameters of the ARES cavity

f_{RF}	508.887	MHz
$U_a : U_s$	1:9	
R/Q	15	Ω
Q	1.1×10^5	
P_c	150	kW Per ARES cavity generating
V_c	0.5	MV (KEKB design)

HOM power is guided through an E-bend waveguide in the horizontal direction, and is finally dissipated in two bullet-shape sintered SiC ceramic absorbers (55 mm in diameter and 400 mm in length including a tapered section) inserted at the end of each waveguide. Each SiC absorber is directly cooled by water flowing in the channel bored inside. The power capability was verified up to 3.3 kW per absorber at a HOM-load test bench with a L-band CW klystron.

Grooving the inner wall of a circular beam pipe can selectively lower the cut-off frequency of the TE_{11} wave, which couples with the dipole modes in the cavity. This is the Grooved Beam Pipe (GBP) method [20], which can heavily damp the dipole modes without deteriorating the accelerating mode impedance. The beam pipe with an inside diameter of 150 mm attached to each end of the accelerating cavity has two grooves at the upper and lower sides in order to damp the dipole modes deflecting the beam in the horizontal direction. The groove dimensions are chosen 30 mm in width and 95 mm in depth, lowering the cut-off frequency of the TE_{11} wave down to 650 MHz. In each groove, there are eight SiC tiles arranged in a line, where the extracted HOM power is dissipated. Each SiC tile is brazed to a water-cooled copper plate with a copper compliant layer between. The GBP HOM load was also tested up to 0.5 kW per groove at the HOM-load test bench. Details of the HOM loads are reported in Ref. [21].

The coupling cavity made of OFC parts is brazed to one side of the accelerating cavity in the horizontal direction. The two cavities are coupled through a rectangular aperture of 120 mm × 160 mm. At the opposite side, another half-cell coupling cavity is brazed for the $\pi/2$-mode termination to restore the symmetry of the accelerating cavity with respect to the mid-vertical plane. Furthermore, the coupling cavity is equipped with a parasitic mode coupler [22] for damping the 0 and π modes down to loaded-Q values of about 100. The parasitic mode coupler is a coaxial line (WX120D) complex with an antenna-type coupler, a disk-type ceramic window, and a cross stub support. The extracted RF power is guided downward through a tapered coaxial line (WX120D-WX77D) toward a water-cooled dummy load with a power capability of 40 kW (CW).

The energy storage cavity operated in the TE_{013} mode is a large cylindrical steel structure with dimensions of 1070 mm in diameter and 1190 mm in axial length, whose inner surfaces are copper plated. The Q value of the TE_{013} mode achieved with the electroplated copper surfaces is 1.65×10^5, which is 85% of the theoretical value assuming a copper electrical conductivity of 5.81×10^7 S/m. The circumferences of both end plates are grooved in order to resolve the degeneracy of the TE_{013} and TM_{113} modes. For compensating thermal detuning, a movable tuning plunger with a diameter of 200 mm and a travel of 60 mm is installed in the central port at the upper end plate, while a fixed tuner placed at the lower end plate. The storage and coupling cavities are coupled through a rectangular aperture of 120 mm × 180 mm, and mechanically connected to rectangular flanges with bolts. Thin stainless-steel lips at the flange connection are to be welded for a vacuum seal in the final stage. For high-power testing above the ground or operation in early commissioning phases, a rubber gasket is to be used instead.

The RF power is fed through an input coupler attached to one of the two drive ports at the middle level of the storage cavity. Two types of input couplers with different window matching structures were developed [23]: the over- and under-cut type, and the choke type. The RF power is transmitted from the rectangular waveguide (WR1500) input via a doorknob transition with a capacitive iris, to the coaxial line (WX152D) with a disk-type ceramic window. The coaxial line is tapered down (WX77D) and ends with a magnetic coupling loop. Both types had been successfully tested up to 950 kW, far above the design power capability of 400 kW.

The production of ARES cavities was started in April 1997. Before installation, every cavity was pre-processed in a high-power test station up to a wall power of 180 kW, 120% of the design power. This limit was due to radiation safety regulations applied to the test station.

6.3. Operational performance

The commissioning of the HER was first started with 6 ARES cavities and four superconducting cavities (SCC) in December 1998, followed by the commissioning of the LER with 12 ARES cavities in January 1999. The typical operational RF voltage in the early stage was 0.4 MV per ARES cavity, 80% of the design voltage. In the summer of 1999, the number of ARES cavities in the LER was increased from 12 to 16 by adding 4 to the RF section D7, and in the HER from 6 to 10 by adding 4 to the RF section D4. Furthermore, every ARES cavity in the LER was vacuum-sealed by welding the thin metal lips at the flange connection after removing the rubber gasket. On the other hand, rubber gaskets are still used for the ARES cavities in the HER. Very high luminosity operation was started in the fall of 1999. The beam currents were increased stepwise, while overcoming many problems with hardware devices and improving the machine performance, some of which have been stated elsewhere. The maximum voltage of the ARES cavity in steady operation was 0.43 MV, generating a total voltage of 6 MV for the LER with 14 cavities at 7 RF stations available out of the 8 RF stations, one of which was not operated due to a cavity vacuum problem.

For each of the 10 ARES cavities installed at the LER RF section D7, the HOM power dissipated in the four bullet-shape SiC absorbers at the downstream side was obtained from the temperature rise of the cooling water flowing through those absorbers in series; the flow rate adjusted in advance. Fig. 6 shows the data obtained for every cavity as a function of the LER beam current in a range from 600 to 900 mA. The bunch pattern was a single train of 1152 bunches with a four-bucket spacing followed by a gap of 512 vacant buckets. The mirror symmetry of the cavity structure with respect to the beam direction assures that twice the power given in Fig. 6 is roughly equal to the total HOM power dissipated in the four rectangular waveguides of each cavity, which amounts to about 1.6 kW at 900 mA. Each curve drawn in Fig. 6 is a fit to the data for each cavity, assuming a quadratic dependence of the HOM power on the beam current. Fig. 7 shows the coefficient of the

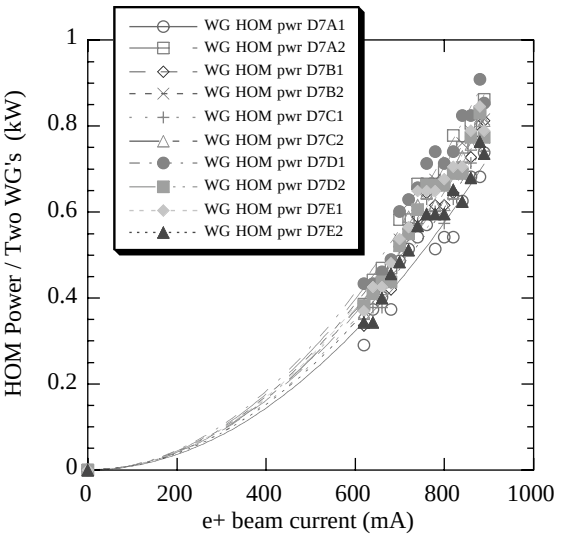

Fig. 6. For every ARES cavity at the RF section D7 in the LER, the HOM power dissipated in the four bullet-shape SiC absorbers at the downstream side is plotted as a function of the beam current.

quadratic term of the beam current obtained from data fitting for every cavity. It can be said that there is a slight tendency for the cavities at both ends of the RF section to have smaller HOM power dissipations. This may be due to higher order modes above the beam pipe cut-off frequency.

Also, the HOM power dissipated at the SiC tiles in the grooved beam pipe at the downstream side of each cavity was obtained in a similar way to that stated above. Fig. 8 shows the data obtained for every cavity at the LER RF section D7. Again, twice the power given in Fig. 8 is roughly equal to the total HOM power dissipated in both grooved beam pipes of each cavity. Fig. 9 shows the coefficient of the quadratic term for every fitted curve in Fig. 8. Comparing Fig. 9 with Fig. 7, then, there can be seen a clear tendency of non-uniformity in the distribution of the HOM power dissipations along the RF section. However, we need a further investigation to confirm this non-uniformity. This is because, unfortunately, the two cavities at the RF station D7C were not operated due to a vacuum problem when the data were taken. An irregular boundary condition, where the storage cavity not exactly tuned to the accelerating

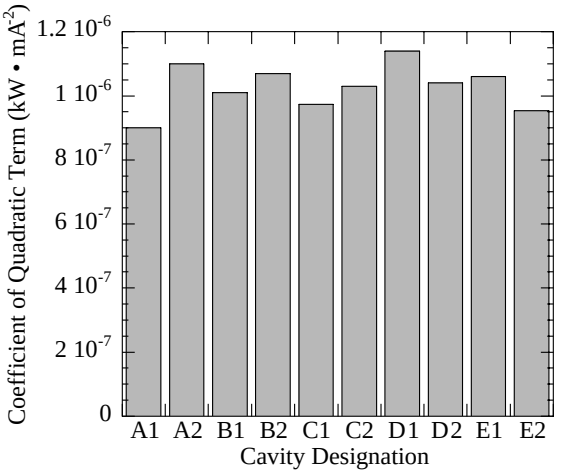

Fig. 7. A graph showing the coefficient of the quadratic term of the beam current, obtained from fitting the HOM power data for each cavity in Fig. 6.

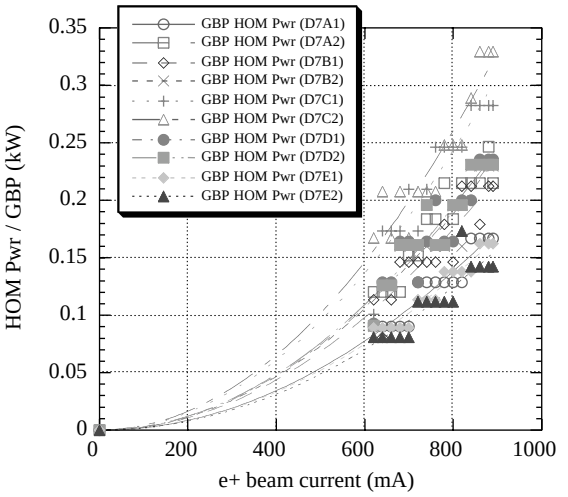

Fig. 8. For every ARES cavity at the RF section D7 in the LER, the HOM power dissipated at the SiC tiles in the grooved beam pipe at the downstream side is plotted as a function of the beam current.

cavity in the $\pi/2$ mode, deforms the accelerating field and may introduce a dipole component around the beam axis.

Through the KEKB operations so far, we have encountered many problems and accidents with the ARES cavities. Those problems can be roughly

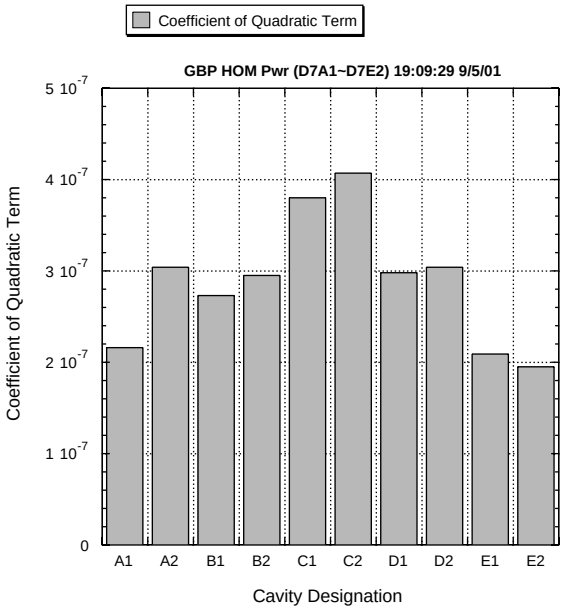

Fig. 9. A graph showing the coefficient of the quadratic term of the beam current, obtained from fitting the HOM power data for each cavity in Fig. 8.

categorized into two groups: infancy problems, especially with accessory devices emerging in a long-term operation with the beam currents being increased stepwise, and cavity problems attributed to quality-control issues, usually incompatible with stringent cost goals in the production phase. Fortunately, none of the problems and accidents had limited the beam current in the LER or the HER. With operational experience accumulated through those difficulties, we are confident of the performance and growth potential of the ARES cavity system toward high-luminosity frontiers explored with the KEKB collider beyond 4.49×10^{33} cm^{-2} s^{-1}.

7. Superconducting cavity

7.1. Introduction

An RF system of the HER is a combination of twelve normal conducting (NC) cavities and eight superconducting (SC) damped cavities, and must supply an accelerating voltage of 8–16 MV and a

beam power of 4 MW. These NC and SC cavities were newly developed to achieve a sufficiently low higher order mode (HOM) impedance to avoid any multibunch instabilities for an ampere-class beam intensity of KEKB. In addition, the frequency detuning of the accelerating mode for minimizing the input RF power must be less than the revolution frequency, 100 kHz in KEKB. If this detuning reaches the revolution frequency, a strong beam instability will be excited and will lose the beam immediately. The frequency detuning δf is in proportion to $(R/Q)/V_c$ described by

$$\delta f = -\frac{I_0 f_{RF}}{2V_c}(R/Q)\sin\phi_s, \quad (1)$$

where I_0, f_{RF}, V_c and ϕ_s are the beam current, the resonant frequency, the accelerating voltage and the synchronous phase. With respect to an SC cavity which can provide a high accelerating voltage and has a cell shape with a rather low R/Q, the detuning can be reduced by one order compared with that of a standard copper cavity. At the same time, the total HOM impedance becomes small, because a smaller number of cavities is sufficient to provide the required RF voltage. From this point of view, the development of an SC damped cavity started in 1991, where optimization of the cavity shape, a HOM damping scheme, and an input coupler of several hundred kW were the main items of R&D for the SC damped cavity system.

The SC damped cavity is essentially the single mode cavity proposed by Weiland [24], where the HOM modes in the cavity propagate out through large beam apertures along the beam axis and are absorbed by dampers located in beam pipes. This cavity shape has a disadvantage of a rather low R/Q for the NC cavity; however, the high Q of the SC cavity can still keep a high shunt impedance (R) of 10^{11} Ohms. The design of cell shape was finished in 1992. A single cell cavity has a beam aperture of 220 mm in diameter to achieve an external Q of 100 for monopole modes, and a cylindrical wave guide of 300 mm in diameter is attached on one side to extract the lowest dipole modes of TE_{11} and TM_{11} [25]. On the other hand, the direct connections of such large apertures to the beam ducts become the source of a large loss factor for a bunch length of 4 mm in KEKB. Therefore, a large diameter of 150 mm is adopted for the beam ducts of the RF sectons and long tapers connect the cavities and ducts to achieve a small loss factor.

Each SC module has IB-004 ferrite absorbers of 300 mm in diameter on one side and 220 mm in diameter on the other side that are bonded on the inner surface of copper beam pipes by HIPping, where sintering and bonding are done simultaneously [26]. The size and the location of these absorbers were carefully optimized both by simulation codes and by measurements as well as the connecting tapers. The input coupler is a coaxial antenna type using a ceramic disk of 152 mm in diameter, and can transfer a traveling RF of 800 kW [27]. The inner and the outer conductors are cooled by water and He gas vapor, respectively. Penetration of the coupler tip into the beam pipe is chosen as 12 mm to obtain an external Q of 7×10^4.

A prototype module was constructed and tested at the TRISTAN Accumulation Ring in 1996. This module accelerated a beam current of 500 mA with a cavity voltage of 1–2 MV, and 350 mA with 2.5 MV (10.3 MV/m). These currents were limited by heating up of other ring components and not by the SC cavity, itself. A peak current of 573 mA was achieved in 16 bunches at an accelerating voltage of 1.2 MV. An RF power of 160 kW was transferred to the beam successfully [28]. In the early stage of this beam test, frequent RF trips occurred due to discharging in the cavity and the coupler, but could be suppressed by improving the vacuum pressure and by coupler conditioning by applying a DC bias voltage to the coaxial conductors.

Construction of the first four SC cavities was started at the end of 1996 and completed in 1998. The existing cryogenics that were used in KEK-TRISTAN, such as a 6.5 kW refrigerator system and the main He transfer line, have been reused. Since the commissioning of KEKB in December of 1998, these cavities have been operated successfully. In the summer of 2000, another four cavities were added. Since then, the RF system of KEKB-HER consists of eight SC cavities in the NIKKO straight section and 10 NC cavities in the OHO

straight section. The maximum current of HER has reached 870 mA so far.

7.2. Design and performance of cavity and its accessories

7.2.1. Cavity

A cross-section view of the KEKB-SC cavity is shown in Fig. 10, and the cavity parameters of the accelerating mode are summarized in Table 6.

The cavity was formed by a spinning method of 2.5 mm Nb sheet of RRR 200. The process of surface treatment using electropolishing was almost the same as that of the TRISTAN cavities. To obtain a carbon-free surface so as to suppress discharging, hydro-preoxide rinsing was replaced by ozonized-ultrapure-water rinsing (OUR). The OUR treatment completely removes any carbon contamination from the electropolished Nb surface. Cold tests of the KEKB cavities showed sufficiently high Q_0 values and a maximum accelerating field of 18.7 MV/m at 4.2 K. An air-exposure test of an OURed test cavity did not show any degradation of the cavity performances; therefore, all of the cavities were rinsed by OUR and exposed to air for 2 days during full assembling into the cryostat. In the test of fully assembled modules, the accelerating field of all cavities reached 10 MV/m after CW processing and by pulse aging, in which a pulse power of 5% duty was added to the CW power level of just below the quench.

One of the most important issues of an SC cavity is an RF trip due to discharging in the cavity and the input coupler region. From the experience of TRISTAN operation, the discharging was caused by a large amount of condensed gas on a cold surface. In a beam test at AR, the prototype cavity frequently tripped by an arcing interlock of the input coupler, which was due to poor vacuum pressure of the beam ducts and a large amount of gas which penetrated into the cavity. This trip rate could be reduced by improving the vacuum pumping system of the beam ducts and by the OUR-treatment of the beam ducts surface. Therefore, beam ducts with the NEG pumps distributed every 60 cm have been

Table 6
Cavity parameters of the KEKB Superconducting cavity

Frequency	508.8	MHz
Gap length	243	mm
Diameter of aperture	220	mm
R/Q	93	Ohms
Geometrical factor	251	Ohms
E_{sp}/E_{acc}	1.84	
H_{sp}/E_{acc}	40.3	Gauss/(MV/m)

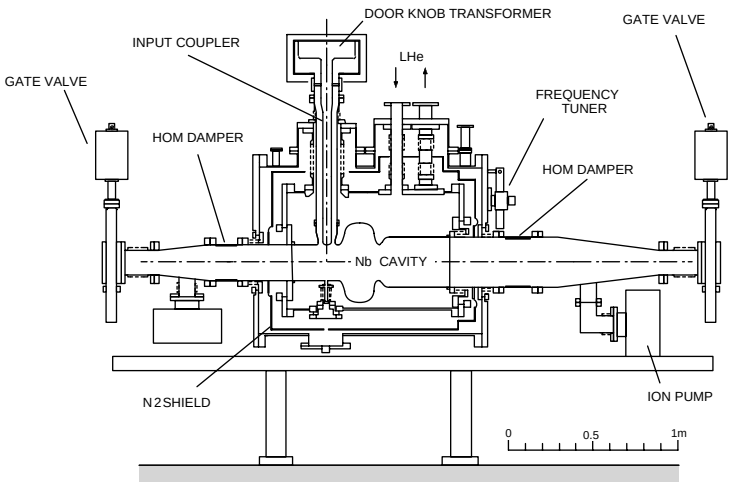

Fig. 10. Input coupler.

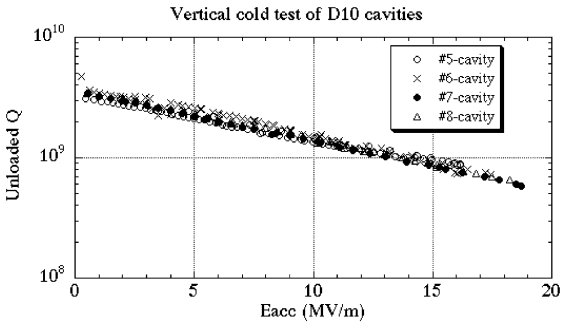

Fig. 11. Vertical measurement.

used to protect the KEKB cavities against any gas from the beam ducts.

The accelerating fields attainable in the cavities were measured using a vertical cryostat. The results were higher than 15 MV/m, as shown in Fig. 11. The accelerating fields decreased to 10–12 MV/m after full assembling, but exceeded the necessary operating field of 6–8 MV/m.

7.2.2. HOM damper

The main part of the HOM losses comes from the tapers between the cavity and the beam ducts. Therefore, the loss parameter of the KEKB cavities was improved from 2.9 V/pC of the AR-prototype cavity to 1.8 V/pC by using beam ducts having a larger diameter and longer tapers, so that the expected power load to the HOM absorbers would be 5 kW per cavity at 1.1 A. The HOM dampers shown in Fig. 12 were made of IB-004 ferrite using a HIP method. Maximum powers of 11.7 and 14.8 kW were successfully given to the 220 mm diameter and the 300 mm diameter dampers at a test stand using a coaxial line with a 508 MHz klystron. In a high-current beam test in AR, the maximum HOM power of 4.2 kW could be absorbed by the HOM dampers without any damage.

7.2.3. Input coupler

The input coupler for KEKB superconducting cavities has almost the same design as that of the TRISTAN cavities. The gap length of 3 mm of the choke structure was increased to 4 mm in order to reduce the field strength at the ceramic disk. To simplify the cooling system of the input coupler,

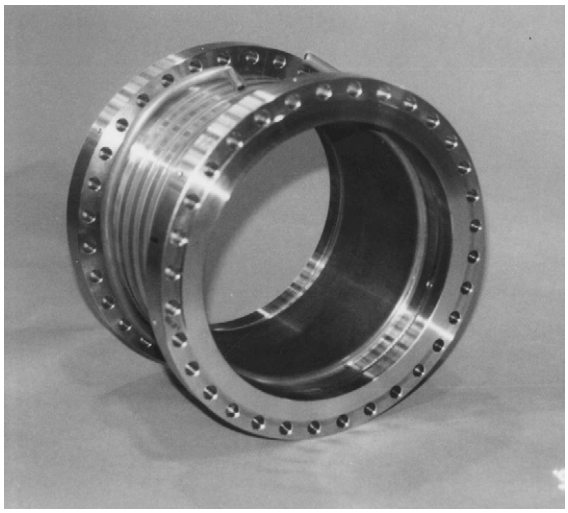

Fig. 12. HOM damper.

the inner conductor is cooled by room-temperature water. The calculated heat transfer by radiation is 0.6 W for an electropolished mirror-like Cu surface. This heat transfer is sufficiently small compared with the total loss of the cavity, and has shown no problem during operation so far, even at a power level of 400 kW. The water flow rate of 1 ℓ/min has a sufficient cooling capacity up to 1 MW. The ceramic window of the coupler is the same as that of 1 MW klystrons, which has shown a long lifetime of more than 50 000 h. However, the KEKB couplers need more diagnostics for precise RF processing and an interlock system for operation under a bad vacuum condition compared to the klystrons. For this purpose, three monitoring ports surround the ceramic window to monitor the vacuum pressure, electrons and discharge light (arc sensor) for protection and diagnosis.

The KEKB couplers were conditioned to 800 kW by traveling waves and a 300 kW totally reflected standing wave, while changing the phase up to a half wave length. At the AR beam test, we developed a biased-type doorknob transition in order to suppress any multipactoring of the input coupler. The inner conductor and the doorknob were electrically isolated by two layers of 0.125 mm thick polyimide film, which produced a capacitance of 1300 pF. A prototype could supply

a power up to 300 kW of both traveling and standing waves without any problem, even for the RF changing phase by a half wave length. The bias-type door-knob transitions for the KEKB cavities has been tested under 450 kW transmission condition, and a 300 kW full reflection condition. A drawing is shown in Fig. 13.

7.3. Operation status

In 1998, four SC cavities were installed at the downstream side of the NIKKO-straight section (D11 side) together with six NC cavities in the OHO-straight section for the HER. Fig. 14 shows the SC cavities at the D11 site. Each SC cavity had been conditioned to 2.5 MV (10 MV/m); however, the commissioning of the HER started with a total RF voltage of 8 MV, and each SC cavity shared a voltage of 1.5 MV. In the first five-month operation for accelerator tuning, the intensity of the HER gradually increased and reached 0.51 A. The SC cavities provided an accelerating voltage of 1.2–2 MV/cavity for various machine studies. The power delivered to the beam by the SC cavities achieved 1.4 MW, which was 40% higher than the design value of 1 MW, and demonstrated a satisfactory performance for the design current of 1.1 A.

In the summer of 2000, another four SC cavities were added at the D10 side of the NIKKO section to improve the beam intensity. Two of them had to be stopped due to a vacuum problem; however, each of the other SC cavities supplied a voltage of 1.4 MV and a 250–300 kW to the beam. Fig. 15, shows the input and reflected power of the D11-A cavity versus the beam intensity. The beam is refilled to keep > 0.6 A during the usual operation; therefore, most of the input power can be transferred to the beam efficiently. This beam loading is adjusted by giving an offset to the cavity phase individually whenever the RF parameters are changed.

The maximum beam intensity of the HER reached 0.78 A in a physics run, and a peak luminosity of 4.49×10^{33} cm^{-2} s^{-1} was achieved. Because of a smaller number of bunches (1153 bunches) with a larger bunch charge of 6.8 nC, as compared with the design profile of 5000 bunches $\times$ 2.2 nC, the induced HOM power has reached the design value of 5 kW in each cavity. In the SC cavity, a wide-range HOM power, which is given as the product of the loss factor, the total

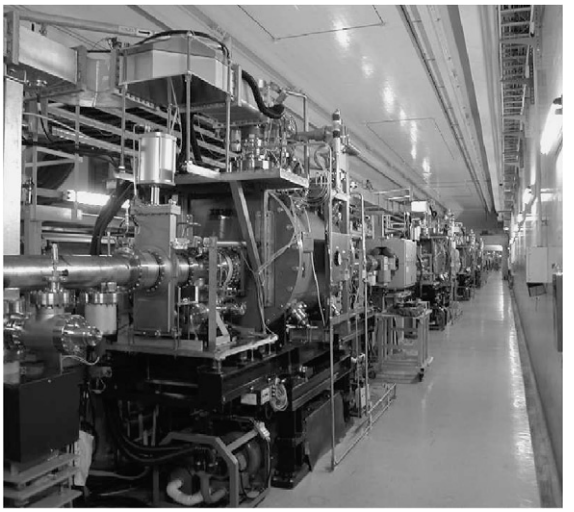

Fig. 14. The SC cavities installed at the D-11.

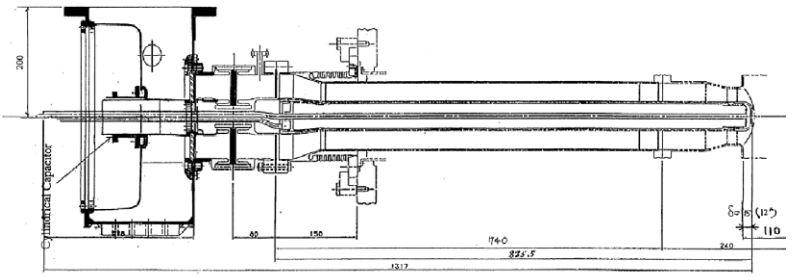

Fig. 13. Input coupler.

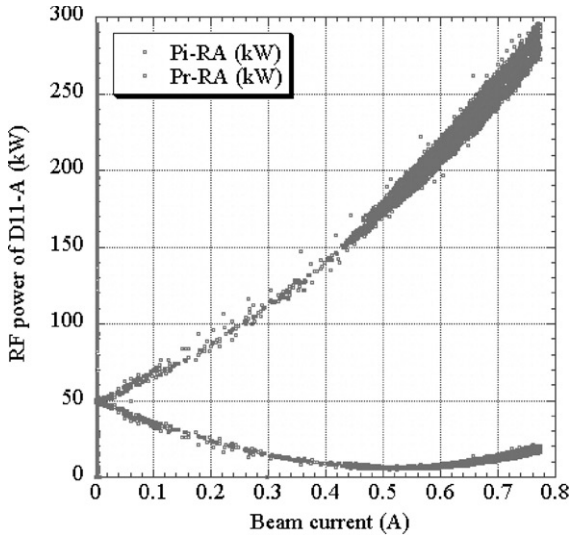

Fig. 15. Input and reflected power of the D11A cavity.

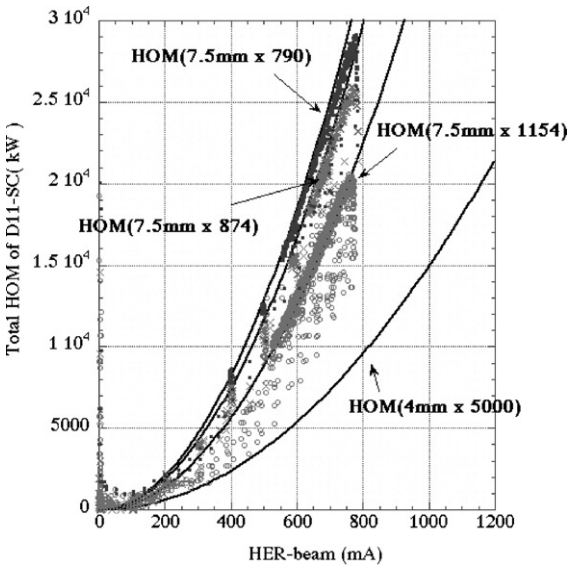

Fig. 16. The result of the HOM power test.

current and the bunch charge, accounts for the most part of the load of the HOM dampers. Since the wide-range HOM power is inversely proportional to the number of bunches, the beam distributed in a larger number of bunches is desired for the HOM dampers. Too much HOM power will raise the surface temperature of ferrite absorbers and bring about a considerable increase in the outgassing. On the other hand, since the positron beam of the LER requires a long bunch spacing of 2.4 m to avoid beam blow up caused by electron clouds, the number of bunches has been reduced to 1153 in both rings so far. Fig. 16 is the result of HOM power tests, in which the total HOM power of the D11 cavities is shown for various bunch numbers of 790, 874 and 1153. The plots obtained from the temperature rise and the flow rate of the cooling water (dots) are in agreement with the power calculated for a bunch length of 7.5 mm (solid lines), which is consistent with that obtained at a bunch-length study. In this test, a maximum HOM power of 7.4 kW was achieved in each cavity without any problem, which corresponded to the power for 1.4 A in 5000 bunches of 4 mm.

The SC cavities tripped several times a day. However, almost all of them occurred when the beam was damped due to various reasons. Because of heavy beam loading, the voltage of the SC cavities drops sharply when the beam is switched off. The SC quench detector recognizes this voltage drop as an SC breakdown, and turns off the RF power. The rate of real breakdown has been less than several times per month. The figures achieved by the SC cavities are summarized in Table 7.

The SC RF system of eight SC damped cavities has been completed in the HER. These cavities have shown good and stable performance, and no beam instability has so far been observed up to 0.87 A of the beam-current. All SC-parameters, such as an accelerating voltage of 2 MV, an RF power to the beam of 380 kW, a HOM power of 7.4 kW and so on, have exceeded our goal values on every SC cavity, and have demonstrated sufficient performance for physics runs at the luminosity of 1×10^{34} cm^{-2} s^{-1}.

8. Superconducting crab cavity

8.1. Crab crossing scheme

For the KEKB beam-crossing, we adopted a finite-angle crossing scheme of 2×11 mrad [1]. By

Table 7
Summary of the figures obtained during operation

	Design	Achieved
Number of SC cavities	8	4 at the commissioning 8 since September 2000
Beam current	1.1 A in 5000 bunches (2.2 nC/bunch)	0.87 A in 1537 bunches (5.7 nC/bunch) 0.78 A in 790 bunches (9.9 nC/bunch)
Bunch length	4 mm	6–8 mm
RF voltage without beam	—	> 2.5 MV/cavity
RF voltage with beam	1.5 MV/cavity	1.2–2.0 MV/cavity
Q value	1×10^9 at 2 MV	$1–2 \times 10^9$ at 2 MV $0.3–1 \times 10^9$ at 2.5 MV
The max. power transferred to the beam	> 250 kW/cavity	370–380 kW/cavity
HOM power	5 kW/cavity at 1.1 A	7.4 kW/cavity at 0.78 A

this scheme, the possibility of a beam–beam instability by a synchrotron–betatron coupling resonance can be anticipated. The crab-crossing scheme shown in Fig. 17 was proposed [29,30] to eliminate these effects. In this scheme, electron and positron bunches to the interaction point are tilted by using a time-dependent strong transverse kick in the superconducting crab cavities to make a head-on collision. After the collision, these bunches are kicked back to the original orientations by other crab cavities.

The R&D program of the KEKB superconducting crab cavity was started in 1994. We have adopted a squashed cell shape for the base line design of the KEKB superconducting crab cavity. This type of the cavity was studied extensively at Cornell in 1991 and 1992 for CESR-B under the KEK-Cornell collaboration [31].

After an R&D study of 1.5 GHz 1/3 scale Nb model cavities [32,33], the fabrication of a full-scale 508 MHz squashed cell shape superconducting crab cavity and a coaxial coupler for the lowest mode damping was started in 1996 [34]. At the same time, a test stand for this cavity, an RF measurement system and a vertical cryostat for a cold test, was constructed.

8.2. Design of crab cavity

Fig. 18 shows the conceptional design of the KEKB superconducting crab cavity. The time-dependent magnetic field on the beam axis by the TM_{110}-like mode is used to obtain time-dependent transverse kick for the crab crossing. In our crab cavity design, by adopting a squashed cell shape cavity we can push up the resonance frequency of the unwanted TM_{110}-like mode, i.e. one other polarization of the crabbing mode, higher than the cut-off frequency of the beampipe, and extract it to outside the cavity. The lowest TM_{010} mode and unwanted higher order modes in the crab cavity are extracted from the cavity through a coaxial coupler and a large aperture beampipe to outside, and are absorbed in RF absorbers attached on both ends of the beam pipes. The head part of the coaxial coupler, which is inserted into a high magnetic field region, must be in a superconducting state. The long inner conductor is supported by a T-stub type structure to obtain mechanical strength. Liquid helium for cooling the inner conductor can be supplied through this support. This coaxial coupler is used for frequency tuning; i.e., by adjusting the insertion depth of the coupler we can easily tune the resonance frequency. A crab-mode rejection notch filter is set to prevent any flowing out of the crabbing mode to the RF absorber.

Fig. 19 shows the full scale 508 MHz squashed cell shape superconducting crab cavity for KEKB. The RF characteristics of this non-axially symmetric shape cavity were calculated by three-dimensional computer code MAFIA. The design maximum electric surface peak field E_{sp}, which corresponds to the required kick voltage of

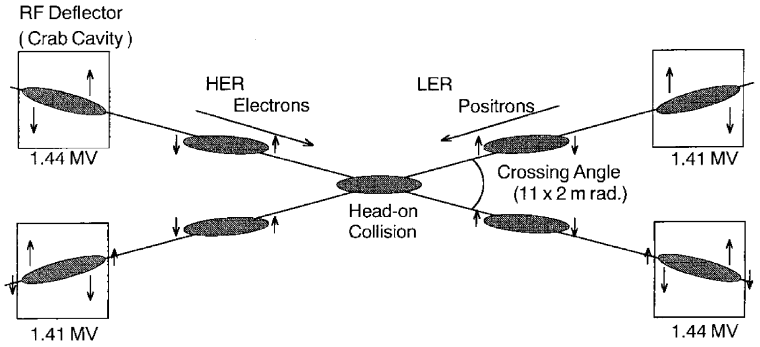

Fig. 17. Crab-crossing scheme of KEKB.

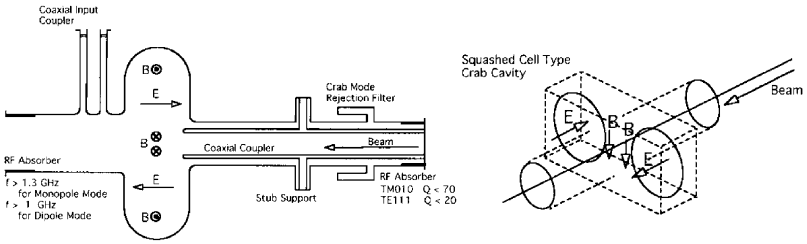

Fig. 18. Conceptional design of the KEKB superconducting crab cavity.

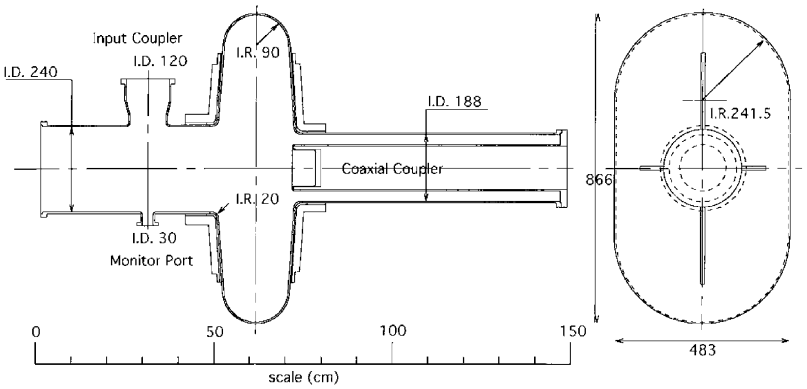

Fig. 19. Full scale 508 MHz squashed cell shape superconducting crab cavity for KEKB.

1.44 MV for the KEKB crab cavities, is about 21 MV/m. The wall thickness of the cavity must be more than 4 mm to withstand an external pressure of 0.13 MPa at room temperature. Also, four ribs for reinforcement are welded to the iris part of the cavity to reduce any stress concentration caused by its non-axially symmetric cell structure.

8.3. Fabrication and surface treatment

The half-cell of the cavity was hydroformed from 5 mm thick Nb sheets with RRR = 190, which were supplied by Tokyo Denkai. The inner surface of the half-cell was buff-polished to remove any scars. The cell and beampipes were assembled into a cavity by electron beam welding.

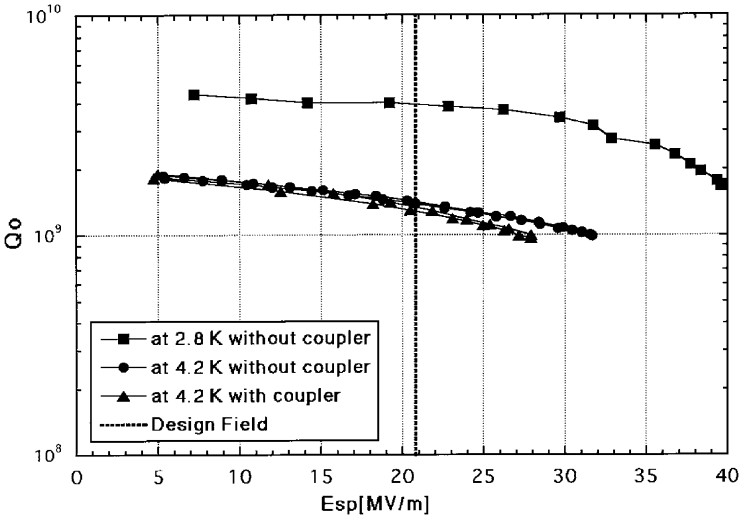

Fig. 20. Q_0 vs. peak surface field E_{sp} value of the KEKB crab cavity without and with coaxial coupler.

The welded equator part of the cell was made smooth by using a specially designed grinding tool. The inner surface of the cavity, especially the equator part, was barrel polished [35] (more than about 200 μm) and then electropolished (about 100 μm). After high-pressure rinsing by 7 MPa ultrapure water, the cavity was annealed in a vacuum furnace at 700° C for 3 h to evacuate any hydrogen gas from the cavity, which was included during electropolishing. The cavity was electropolished slightly and high-pressure rinsed, and then assembled into the vacuum system for the cold test.

An inner conductor of the simplified coaxial coupler was designed and fabricated from Nb. This is to be used in a performance test of the crab cavity in a vertical cryostat.

8.4. Test results

Performance tests of the full scale crab cavity were carried out in a vertical cryostat at 4.2 and 2.8 K. Fig. 20 shows the Q_0 vs. peak surface field E_{sp} of the crab cavity without and with coaxial coupler. In our crab-cavity design a possibility of multipacting at insertion part of the coaxial coupler was anticipated. Although we observed the multipacting phenomena at a very low RF field, we could overcome this by RF processing for about 30 min. We could attain a maximum electric surface peak field E_{sp} of about 32 MV/m with a Q_0 value of 10^9 for the crab cavity. In the case that a coaxial coupler was installed into the cavity, an E_{sp} of about 27 MV/m with a Q_0 value of 10^9 was obtained. This performance exceeded the design E_{sp} of about 21 MV/m with a Q_0 value of 10^9.

The following is a summary of this section. We have designed and fabricated a full-scale 508 MHz squashed cell shape superconducting Nb crab cavity and a coaxial coupler for the lowest mode damping for KEKB. A maximum electric surface peak field E_{sp} of about 27 MV/m at a Q_0 value of 10^9, higher than the design value of about 21 MV/m, was obtained with a coaxial coupler. We could thus establish fabrication and surface-treatment techniques for non-axially symmetric squashed cell shape superconducting Nb crab cavities for KEKB. A design study of the jacket-type horizontal cryostat for KEKB is now underway for constructing a prototype KEKB superconducting crab cavity.

9. Conclusions

The ARES and the SCC, both of which are originally designed HOM damped high-stored-energy cavities, have worked very well with very

large stored beam currents. Klystrons, power supplies and waveguide components including newly developed 1.2 MW water-loads performed very well during physics runs. The low-level control system, which includes many new feedback loops, has well stabilized the RF and the beam, and has contributed to keeping the physics runs stable. As a whole, the RF system has performed very well and has no fundamental difficulties in reaching the design beam currents. The development of the superconducting crab cavity has progressed sufficiently; a full-scale prototype cavity has well exceeded the design deflecting field.

Acknowledgements

The authors would like to thank Professors K. Oide, S. Kurokawa and Y. Kamiya for their encouragement and supporting the design, construction and operation of the RF systems. They are also very grateful to Dr. E. Kikutani for performing the editorial task.

References

[1] KEK B-Factory Design Report, KEK Report 95-7, August 1995.
[2] T. Kageyama, et al., Proceedings of the First Asian Particle Accelerator Conference, Tsukuba, Japan, 1998, p. 773.
[3] T. Furuya, et al., Proceedings of the Ninth Workshop on RF Superconductivity, Santa Fe, NM, 1999, p. 31.
[4] Y. Arisumi, et al., Proceedings of the 12th Symposium on Accelerator Science and Technology, Wako, Japan, 1999, p. 266.
[5] S. Isagawa, Proceedings of the 11th Symposium on Accelerator Science and Technology, Harima, Japan, 1997, p. 185.
[6] S. Isagawa, et al., Proceedings of the First Asian Particle Accelerator Conference, Tsukuba, Japan, 1998, p. 773.
[7] E. Ezura, et al., Proceedings of the First Asian Particle Accelerator Conference, Tsukuba, Japan, 1998, p. 770.
[8] K. Ebihara, et al., Proceedings of the 12th Symposium on Accelerator Science and Technology, Wako, Japan, 1999, p. 212.
[9] E. Ezura, et al., Proceedings of the International Workshop on Collective Effects and Impedance for B-Factories, Tsukuba, 1995, p. 437.
[10] K. Akai, et al., Proceedings of the Sixth European Particle Accelerator Conference, Stockholm, 1998, p. 1749.
[11] K. Akai, et al., Proceedings of the 11th Symposium on Accelerator Science and Technology, Harima, 1997, p. 179.
[12] K. Akai, et al., Proceedings of the Fifth European Particle Accelerator Conference, Stockholm, 1996, p. 1994.
[13] T. Ieiri, et al., Proceedings of the Particle Accelerator Conference, Chicago, 2001, p. 2432.
[14] Y. Funakoshi, Proceedings of the Mini-Workshop on KEK B-Factory, KEK, Japan, July 1991.
[15] T. Shintake, Particle Accelerators 44 (1994) 131.
[16] I. Wilson, H. Henke, CERN 89-09, 1989.
[17] Y. Yamazaki, T. Kageyama, Particle Accelerators 44 (1994) 107.
[18] T. Kageyama, et al., Proceedings of the Particle Accelerator Conference, Vancouver, Canada, 1997, p. 2902.
[19] N. Akasaka, et al., Proceedings of the Particle Accelerator Conference, Dallas, TX, 1995, p. 1738.
[20] T. Kageyama, Proceedings of the 15th Linear Accelerator Meeting in Japan, Sapporo, 1990, p. 79, and Proceedings of the Eighth Symposium on Accelerator Science and Technology, Wako, Japan, 1991, p. 116.
[21] Y. Takeuchi, et al., Proceedings of the Particle Accelerator Conference, Vancouver, Canada, 1997, p. 2986.
[22] F. Naito, et al., Proceedings of the Particle Accelerator Conference, Vancouver, Canada, 1997, p. 2977.
[23] F. Naito, et al., Proceedings of the Asian Particle Accelerator Conference, Tsukuba, Japan, 1998, p. 776.
[24] T. Weiland, DESY 83-073, 1983.
[25] T. Takahashi, et al., Proceedings of the Ninth Symposium on Accelerator Science and Technology, KEK, Japan, 1993, p. 327.
[26] T. Tajima, Thesis, KEK Report 2000-10, September 2000.
[27] S. Mitsunobu, et al., Proceedings of the Seventh Workshop of RF Superconductivity, CEA-Saclay, France, 1995, p. 735.
[28] T. Furuya, et al., Proceedings of the Particle Accelerator Conference, Vancouver, Canada, 1997, p. 3087.
[29] R.B. Palmer, SLAC-PUB 4707, 1988.
[30] K. Oide, K. Yokoya, Phys. Rev. A 40 (1989) 315.
[31] K. Akai, et al., Proceedings of the Particle Accelerator Conference, Washington, DC, 1993, p. 769.
[32] K. Hosoyama, et al., Proceedings of the Seventh Workshop on RF Superconductivity, CEA-Saclay, France, 1995, p. 671.
[33] Y. Morita, et al., Proceedings of the Eighth Workshop on RF Superconductivity, Padova, Italy, 1997, p. 540.
[34] K. Hosoyama, et al., Proceedings of the Eighth Workshop on RF Superconductivity, Padova, Italy, 1997, p. 547.
[35] T. Higuchi, et al., Proceedings of the Seventh Workshop on RF Superconductivity, CEA-Saclay, France, 1995, p. 723.